Report

Neuron

Human *C9ORF72* Hexanucleotide Expansion Reproduces RNA Foci and Dipeptide Repeat Proteins but Not Neurodegeneration in BAC Transgenic Mice

Highlights

- Mouse model expressing ALS/FTD associated C9ORF72 hexanucleotide repeat expansion
- Formation of sense and antisense C9ORF72 RNA transcript foci
- Dipeptide repeat proteins produced by repeat-associated non-ATG translation
- Formation of cytoplasmic inclusions containing dipeptide repeat proteins

Authors

Owen M. Peters, Gabriela Toro Cabrera, Helene Tran, ..., Leonard Petrucelli, Christian Mueller, Robert H. Brown, Jr.

Correspondence

chris.mueller@umassmed.edu (C.M.), robert.brown@umassmed.edu (R.H.B.)

In Brief

Peters et al. report that transgenic mice expressing ALS/FTD-associated C9ORF72 hexanucleotide expansions develop histopathological features of c9ALS/FTD (RNA foci and aggregates of non-ATG translated dipeptides) but not motor neuron disease. These features are attenuated in vitro by anti-C9ORF72 microRNA.

Accession Number

GSE74973

Peters et al., 2015, Neuron *88*, 902–909
December 2, 2015 ©2015 Elsevier Inc.
http://dx.doi.org/10.1016/j.neuron.2015.11.018

CellPress

Neuron
Report

Human *C9ORF72* Hexanucleotide Expansion Reproduces RNA Foci and Dipeptide Repeat Proteins but Not Neurodegeneration in BAC Transgenic Mice

Owen M. Peters,[1,8] Gabriela Toro Cabrera,[1,2,8] Helene Tran,[1] Tania F. Gendron,[3] Jeanne E. McKeon,[1] Jake Metterville,[1] Alexandra Weiss,[1] Nicholas Wightman,[1] Johnny Salameh,[1] Juhyun Kim,[7] Huaming Sun,[2] Kevin B. Boylan,[4] Dennis Dickson,[3] Zachary Kennedy,[1] Ziqiang Lin,[1] Yong-Jie Zhang,[3] Lillian Daughrity,[3] Chris Jung,[6] Fen-Biao Gao,[1] Peter C. Sapp,[1,5] H. Robert Horvitz,[5] Daryl A. Bosco,[1] Solange P. Brown,[7] Pieter de Jong,[6] Leonard Petrucelli,[3] Christian Mueller,[2,*] and Robert H. Brown, Jr.[1,*]

[1]Department of Neurology, University of Massachusetts Medical School, Worcester, MA 01655, USA
[2]Department of Pediatrics and Horae Gene Therapy Center, University of Massachusetts Medical School, Worcester, MA 01655, USA
[3]Department of Neuroscience
[4]Department of Neurology
Mayo Clinic, 4500 San Pablo Road, Jacksonville, FL 32224, USA
[5]Department of Biology, McGovern Institute for Brain Research, and Howard Hughes Medical Institute, 77 Massachusetts Avenue, Massachusetts Institute of Technology, Cambridge, MA 02139, USA
[6]Children's Hospital Oakland Research Institute, 5700 Martin Luther King Jr Way, Oakland, CA 94609, USA
[7]Solomon H. Snyder Department of Neuroscience, Johns Hopkins University School of Medicine, Baltimore, MD 21205, USA
[8]Co-first author
*Correspondence: chris.mueller@umassmed.edu (C.M.), robert.brown@umassmed.edu (R.H.B.)
http://dx.doi.org/10.1016/j.neuron.2015.11.018

SUMMARY

A non-coding hexanucleotide repeat expansion in the *C9ORF72* gene is the most common mutation associated with familial amyotrophic lateral sclerosis (ALS) and frontotemporal dementia (FTD). To investigate the pathological role of *C9ORF72* in these diseases, we generated a line of mice carrying a bacterial artificial chromosome containing exons 1 to 6 of the human *C9ORF72* gene with approximately 500 repeats of the GGGGCC motif. The mice showed no overt behavioral phenotype but recapitulated distinctive histopathological features of *C9ORF72* ALS/FTD, including sense and antisense intranuclear RNA foci and poly(glycine-proline) dipeptide repeat proteins. Finally, using an artificial microRNA that targets human *C9ORF72* in cultures of primary cortical neurons from the C9BAC mice, we have attenuated expression of the C9BAC transgene and the poly(GP) dipeptides. The *C9ORF72* BAC transgenic mice will be a valuable tool in the study of ALS/FTD pathobiology and therapy.

INTRODUCTION

Amyotrophic lateral sclerosis (ALS) is a neurodegenerative disease that primarily affects motor neurons in the motor cortex, brainstem, and spinal cord; frontotemporal dementia (FTD) is caused by the degeneration of neurons in the fronto-temporal regions. Some individuals develop ALS and FTD simultaneously. Our understanding of these diseases was transformed by the identification in some ALS/FTD cases of an abnormally expanded GGGGCC repeat motif within the gene chromosome 9 open reading frame 72 (*C9ORF72*) (DeJesus-Hernandez et al., 2011; Gijselinck et al., 2012; Renton et al., 2011). Now recognized as the most common cause of dominantly inherited ALS and FTD (c9ALS/FTD), the *C9ORF72* GGGGCC motif can be expanded to several thousand repeats in affected individuals (Majounie et al., 2012).

The normal function of the *C9ORF72* product is unknown, though a role in membrane trafficking has been suggested (Farg et al., 2014). Decreased levels of *C9ORF72* transcripts have been described in c9ALS/FTD patient tissues and derived cell lines (Belzil et al., 2013; DeJesus-Hernandez et al., 2011), suggesting that haploinsufficiency might contribute to disease. It is also likely that the intronic *C9ORF72* repeat expansion confers one or more toxic properties that compromise neuron viability. Bidirectional transcription of the mutated *C9ORF72* generates GGGGCC sense and CCCCGG antisense repeat-containing RNA transcripts that form intranuclear RNA foci (Mizielinska et al., 2013) and potentially sequester RNA binding proteins (Cooper-Knock et al., 2014). The expanded RNA transcripts also undergo repeat-associated non-ATG (RAN) translation, a non-canonical mechanism of protein synthesis that yields aggregation-prone dipeptide repeat (DPR) proteins that form cytoplasmic inclusion bodies (Ash et al., 2013; Mori et al., 2013; Zu et al., 2011).

Model systems that recapitulate the pathobiology of the mutant *C9ORF72* gene are particularly helpful in understanding how such mutations cause neurodegeneration in vivo. Several invertebrate (Mizielinska and Isaacs, 2014; Therrien et al., 2013; Tran et al., 2015), vertebrate (Ciura et al., 2013; Chew et al., 2015), and patient-derived cell models (Almeida et al., 2013; Donnelly et al.,

2013; Lagier-Tourenne et al., 2013; Sareen et al., 2013) of *C9ORF72* motor neuron pathology have been reported. While each of these models have been instructive, it can be argued that a more informative model will permit studies of the *C9ORF72*-expanded GGGGCC repeats in the context of stable expression in an intact mammalian nervous system. For that reason, we have generated a novel transgenic mouse carrying an expanded form of the human *C9ORF72* gene with approximately 500 GGGGCC motifs.

RESULTS

BAC Transgenic Mice Express the Human Mutant *C9ORF72* Gene

We generated a line of SJL/B6 transgenic mice using a 153.2 kb bacterial artificial chromosome containing exons 1 through 6 of the human *C9ORF72* with about 500 GGGGCC repeat motifs, including approximately 140.5 kb of upstream sequence (Figure 1A; Figure S1A). Hemizygous C9BAC mice were viable, producing progeny at expected Mendelian frequencies. Southern blot analysis of genomic DNA from these animals detected two distinct bands corresponding to about 500 and 300 GGGGCC repeat motifs, which were intergenerational (Figure S1B) and tissue-type stable (Figure 1B). Using a human-specific probe for all variants (Vall), *C9ORF72* mRNA transcripts were detected in the C9BAC mice in all tissues examined (Figure S1C). The truncated human *C9ORF72* gene generates three transcript variants; V1 and V3 carry the repeat expansion (Figure S1A). Human-specific probes targeting human *C9ORF72* V1, V2, and V3 mRNAs detected all three transcripts in the C9BAC mice at expression levels relative to their abundances in human frontal cortex (Figure 1C). Moreover, the total level of the transgenic human transcripts was roughly comparable to that of the endogenous mouse *C9ORF72* ortholog transcripts and to levels of expression of human control and c9ALS/FTD cases (Figure 1C).

Survival, Motor, and Cognitive Systems Are Normal in Mice Bearing the Mutant *C9ORF72* Gene

A cohort of F1 generation male C9BAC mice was aged for phenotypic characterization and analysis of survival. At all ages, the C9BAC and control mice remained healthy. They trended toward a non-significantly elevated weight compared to non-transgenic (Ntg) littermates (Figure S1D) and lived beyond 2 years. Survival in the C9BAC and Ntg littermates was indistinguishable (Figure 1D).

We first tested for behavioral and histological abnormalities within the motor system of the C9BAC mouse. Overall, the C9BAC mice showed no significant motor deficits by rotarod performance and grip strength testing (Figures S1E and S1F). No difference was observed in motor or sensory spinal nerve root axon number and morphology (Figure S2A), nor was increased denervation of neuromuscular junctions seen in 24-month-old C9BAC mice (Figure S2B). Motor unit number estimation (MUNE) recording in the hind limbs of 24-month-old C9BAC mice detected no changes in MUNE score, motor unit size, or compound motor action potential, although there was a trend toward a modestly increased denervation score, as gauged by electromyography (Figure 1E).

We also assessed several pathological features in the motor cortex and spinal cord that are common features of ALS. No significant changes were seen in activation of microgliosis or astrogliosis (Figures S2C and S2E). Cytoplasmic mislocalization and aggregation of TDP-43, both identified in the majority of ALS patients (Janssens and Van Broeckhoven, 2013; Rohrer et al., 2015), were not detected in the motor cortex of our C9BAC mice (Figures S2D and S2E). To assess activation of programmed cell death within the spinal cord, we observed levels of cleaved capase-3 by western blotting; levels in C9BAC and Ntg mice did not differ significantly (Figure S2F). Because studies have demonstrated cortical hyperexcitability in ALS patients and cell lines with *C9ORF72* hexanucleotide expansions (Geevasinga et al., 2015), we next asked whether cortical neurons of neonatal C9BAC mice showed altered electrophysiological characteristics. We detected no changes in the electrophysiological properties of either pyramidal tract-type or intratelencephalically projecting neurons in L5 of motor cortex of these neonatal C9BAC mice (Figures S2G–S2J; Table S1).

We next surveyed pathological findings that are common in FTD. No activation of gliosis was detected in the prefrontal cortex (PFC) or hippocampus (Figures S3A and S3B). Changes in social interaction behavior have been described in rodent models of FTD (Alfieri et al., 2014; Gascon et al., 2014); however, we found no change in social behavior of adult C9BAC in response to an intruder mouse assay. (Figure S3C). Quantitative studies of Golgi preparations revealed no change in dendritic spine density of PFC layer 2-3 pyramidal neuron apical dendrites in aged C9BAC mice (Figure S3D). Finally, altered gene expression profiles have been shown in c9ALS/FTD patient-derived cell lines (Donnelly et al., 2013; Lagier-Tourenne et al., 2013; Sareen et al., 2013) and tissues (Prudencio et al., 2015). To determine whether a specific *C9ORF72* RNA profile can be defined in our C9BAC transgenic mice, we sequenced total RNA extracted from the frontal cortex of 6-month-old C9BAC mice and littermate controls. Statistical analysis of differentially expressed genes did not reveal any change between the two groups, including several genes identified as differentially expressed in induced pluripotent stem cell (iPSC)-derived motor neurons (Donnelly et al., 2013; Sareen et al., 2013) (Figures S3E–S3H).

C9BAC Mice Recapitulate Histopathological Features of Human *C9ORF72* ALS-FTD

At autopsy, brains from c9ALS/FTD patients show several histopathological characteristics that are not detected in other forms of familial and sporadic ALS or FTD: (1) sense transcript nuclear and occasional cytoplasmic RNA foci, (2) antisense transcript nuclear RNA foci, and (3) the generation of DPR proteins through RAN translation of the sense and antisense transcripts.

We used fluorescence in situ hybridization (FISH) to detect *C9ORF72* sense and antisense foci in the brain and spinal cord of C9BAC mice (Figure 2). Intranuclear, sense foci were detected at 3 months of age (data not shown) and by 10 and 24 months were abundant throughout the CNS, including motor cortex and spinal cord (Figure 2A), present in both neurons (Figures 2B and 2C), and glia (Figure 2D). Antisense foci were also detected in 10- and 24-month-old mice (Figure 2A) but were more sparse throughout the brain than sense foci. Quantification

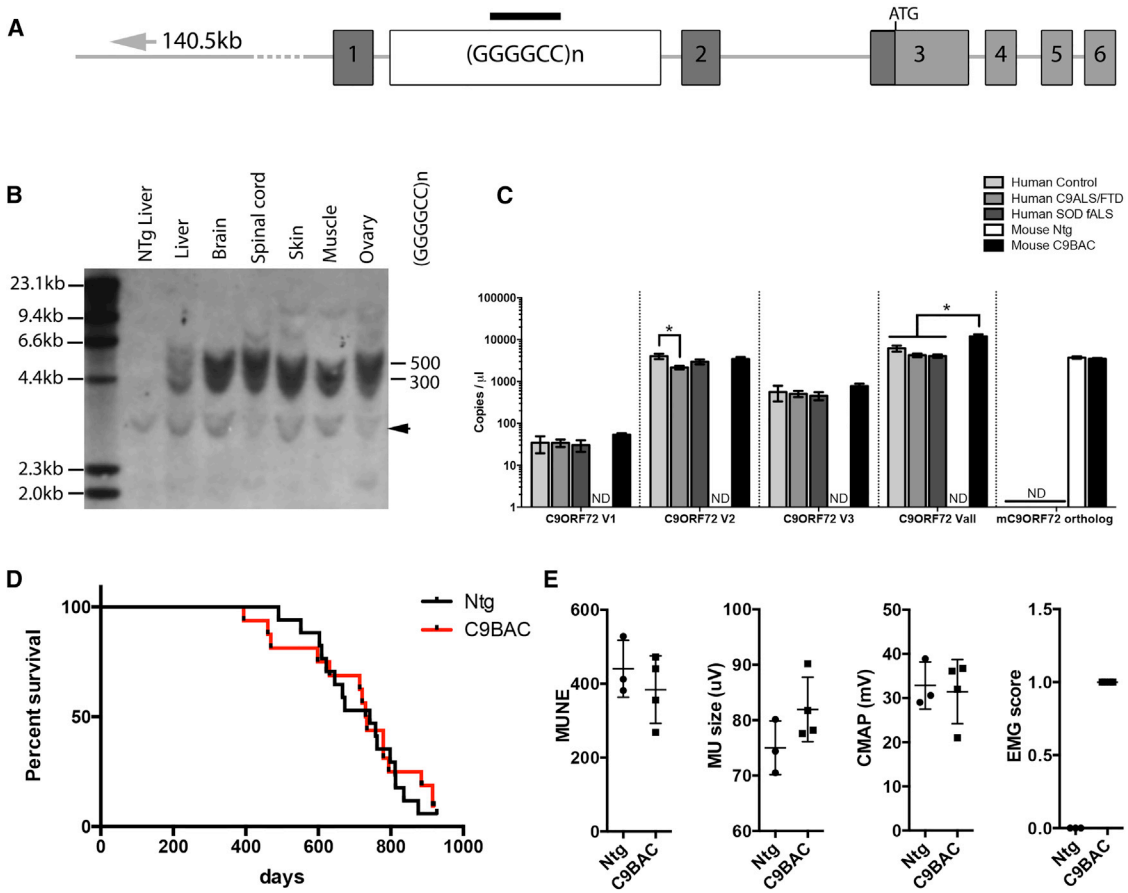

Figure 1. Construct Design, Expansion Size, and Expression Profile for the *C9ORF72* BAC Transgene and Phenotyping of C9BAC Mice

(A) Schematic of the bacterial artificial chromosome fragment used for generating the C9BAC mice. The 153.2 kb construct contains (as shown from left to right) 140.5 kb of human genomic DNA upstream of *C9ORF72*, the human *C9ORF72* promoter region, and exons 1 to partial exon 6 with a $(GGGGCC)_{500}$ repeat motif in *C9ORF72* intron 1. The black bar indicates the target region for the Southern blotting probe used in (B).

(B) Southern blot of genomic DNA extracted from various tissues digested with HindIII, SacI, and TaqI and probed with a 5′-DIG-$(GGGGCC)_5$-DIG-3′ DNA probe. Two bands of ~4.4 kb and ~6.0 kb are stable in size after six generations representing expansions of 300 and 500 repeats (see also Figure S1B). The arrowhead indicates a non-specific band.

(C) ddPCR analysis of expression of all human *C9ORF72* variants (Vall), and variants V1, V2, and V3 and the mouse *C9ORF72* ortholog in human frontal cortex tissues from non-neurological disease control, c9ALS/FTD and SOD fALS patients, and whole-brain homogenate from C9BAC and Ntg mice (mean ± SEM, n = 4, Kruskal-Wallis test, Mann-Whitney U test, *$p < 0.05$, ND = not detectable).

(D) Kaplan-Meier curve representing lifespan showing no significant difference in survival of C9BAC mice compared to Ntg littermates (Ntg n = 17, C9BAC n = 16, Mandel-Cox Log Rank, $p = 0.971$).

(E) Physiological studies reveal showed no significant change in motor unit number estimations (MUNEs), motor units size, or compound motor action potential, though a modest increase in electromyogram score was observed (mean ± SEM, Ntg n = 3, C9BAC n = 4 unpaired t test).

of numbers of sense foci in nuclei of the cortical internal pyramidal layer (layer V) (Figure 2E) and spinal motor neurons (Figure 2F) revealed that the majority of foci-positive nuclei contain one to five detectable sense foci, though in some cases greater than 20 foci were seen in individual nuclei. A trend toward a reduced number of nuclei containing foci was seen between 10 and 24 months, reaching statistical significance in the motor cortex internal pyramidal layer, but not spinal cord motor neurons.

Because both sense and antisense *C9ORF72* transcripts were present in the C9BAC mice, we next sought evidence of RAN translation products, using a sandwich immunoassay for the detection of poly(Glycine-Proline) (poly(GP)), which is synthesized from both sense and antisense transcripts. Tissues from 4- and 24-month-old Ntg and C9BAC mice, and frontal cortex from six c9ALS cases, were homogenized in buffer containing 2% SDS, with the detergent-soluble fraction analyzed for poly(GP) content. At 4 months of age, poly(GP) was detected throughout the brain of C9BAC mice, with levels highest in the cerebellum, and also detected in the spinal cord, sciatic nerve, and liver (Figure 2G). Though the mean concentration of poly(GP) levels in 4-month-old mice was lower than that observed in c9ALS frontal cortex, the 4-month-old C9BAC mean did fall within range of the lowest samples in the patient group (Figure 2G). All tissues from 24-month-old C9BAC mice showed a significant reduction in SDS-soluble poly(GP) levels. One hypothesis for the observed decline in soluble poly(GP) is that the

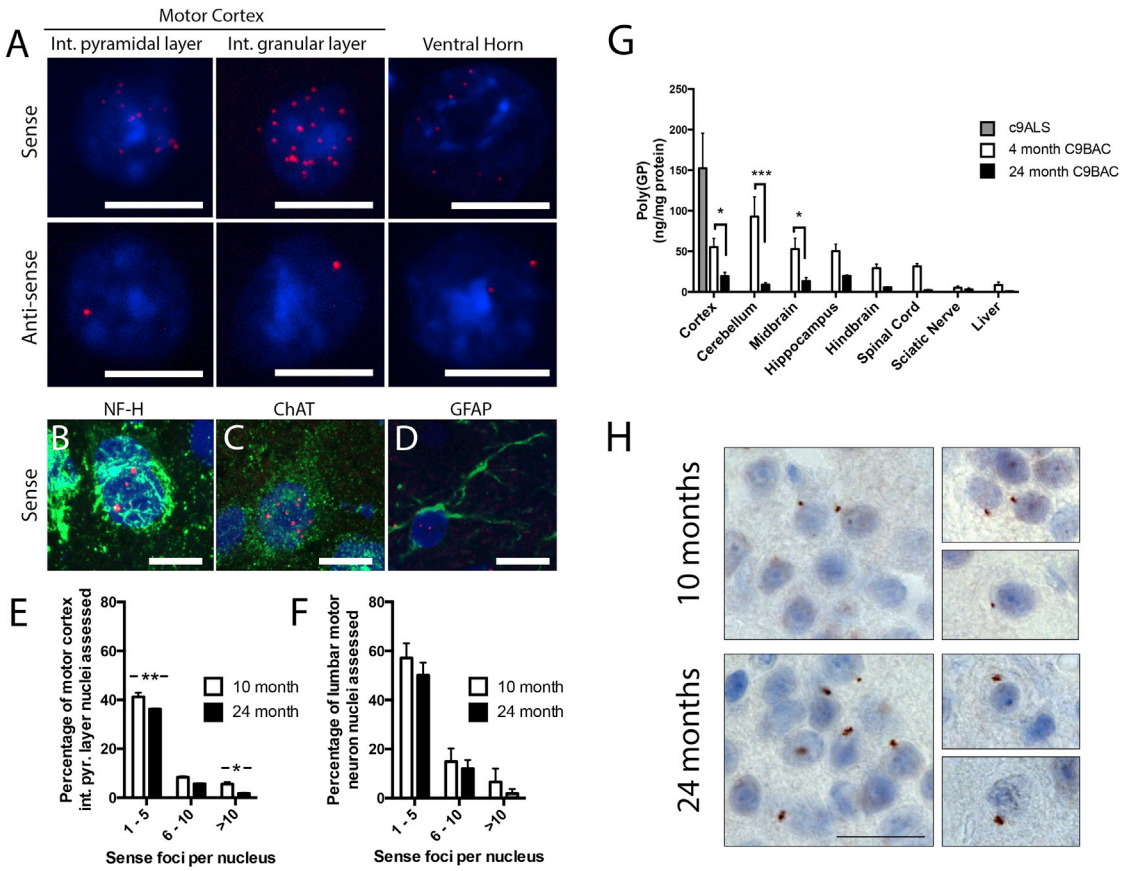

Figure 2. C9BAC Mice Recapitulate the Histopathological Hallmarks of *C9ORF72* ALS and FTD Patients

(A) Fluorescence in situ hybridization (FISH) using Cy3-tagged DNA probes against sense and antisense abnormally expanded *C9ORF72* transcripts (red, probe; blue, DAPI nuclear stain). The *C9ORF72* repeat containing sense or antisense transcripts form intranuclear RNA inclusions, or foci, throughout the brain, including motor cortex internal pyramidal layer and internal granular layer, and lumbar motor neurons of 24-month-old C9BAC mice.

(B–D) FISH coupled with cell-type-specific immunostaining revealed sense transcript foci in neurofilament heavy-positive neurons (B), choline acetyl transferase (ChAT)-positive pyramidal neurons (C), and GFAP-positive astrocytes (D).

(E and F) The number of sense transcript foci per nucleus in 10-month- and 24-month-old C9BAC mice in (E) motor cortex internal pyramidal layer and (F) lumbar motor neuron nuclei (cortex: 10-month, n = 3, 821 nuclei; 24-month, n = 3, 845 nuclei: spinal cord: 10-month, n = 3, 124 nuclei; 24-month, n = 3, 100 nuclei: mean ± SEM, two-way ANOVA, Bonferroni multiple comparison *$p < 0.05$, **$p < 0.001$).

(G) Quantification of soluble poly(GP) proteins in various regions of the CNS and liver of 4- and 24-month-old C9BAC mice and frontal cortex of c9ALS cases by immunoassay (mean ± SEM, C9BAC groups n = 3, c9ALS n = 6, two-way ANOVA, Bonferroni's multiple comparison, *$p < 0.05$, ***$p < 0.001$).

(H) Immunostaining for poly(GP) proteins in cortex of C9BAC mice. Staining revealed the presence of small perinuclear inclusion bodies throughout the brain at 10 months of age, with a pronounced elevation in the number observed in 24-month-old mice. Such inclusions were not observed in age-matched Ntg mice. Scale bars: (A)–(D) = 10 μm; (H) = 20 μm.

DPR proteins show an age-dependent propensity to form insoluble species. Immunostaining of brain tissues from 10- and 24-month-old C9BAC mice revealed the presence of small perinuclear inclusion bodies stained for poly(GP) (Figure 2H). Such inclusions were detected throughout the brain, including cortex, cerebellum, and striatum, and were more frequently observed in the brains of 24-month-old mice, suggesting a heightened deposition of insoluble poly(GP) species.

We established primary cortical neuron cultures from C9BAC and Ntg littermate embryos. At 10 days in vitro (DIV), both nuclear foci containing sense or antisense *C9ORF72* hexanucleotide expansion transcripts (Figure 3A) and poly(GP) RAN translation products could be detected (Figure 3B). We next tested whether neurons from C9BAC mice are hypersensitive to cellular stress. In a previous study, neuron-differentiated iPSCs derived from FTD patients showed an increased sensitivity to cell death induced by inhibition of autophagy in vitro (Almeida et al., 2013). We treated DIV15 primary cortical neuron cultures derived from individual embryos with two inhibitors of autophagy (Figure 3C), chloroquine and 3-methyladenine. Both compounds increased cell death to the same degree in the C9BAC and Ntg neurons, as determined by an LDH assay.

Silencing *C9ORF72* Transcripts and Poly(GP) Production In Vitro

Though lacking cognitive or motor deficits, the C9BAC mouse robustly recapitulates the molecular pathology of c9ALS/FTD, with readily quantifiable expression of all three *C9ORF72*

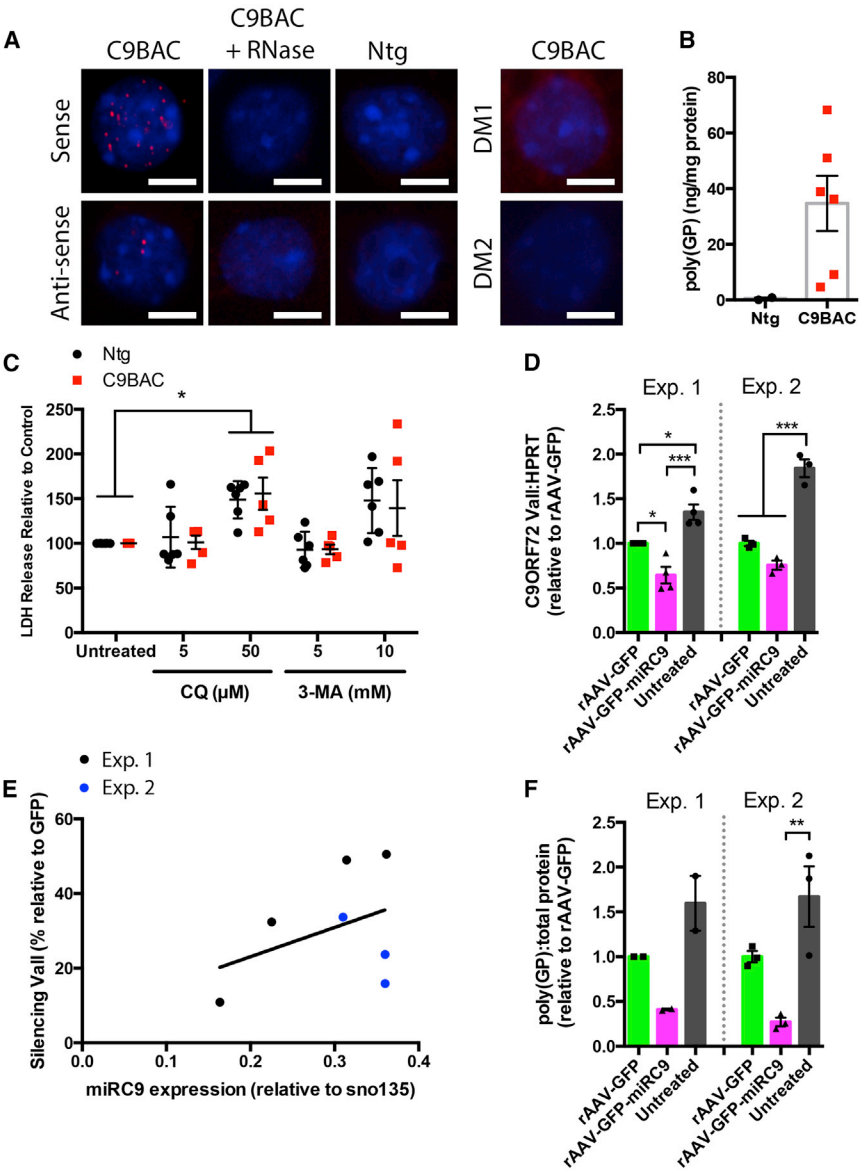

Figure 3. Silencing of *C9ORF72* in C9BAC Mice and Primary Cortical Neurons

(A) Sense and antisense foci are detected in cultured cortical neurons of C9BAC embryos at 10 days in vitro (DIV). These foci were not visible following RNase treatment and were not detected in Ntg neurons or by probes targeting the myotonic dystrophy-associated type-1 (CTG)n or type-2 (CCTG)n expansions (DM1 and DM2, respectively, scale bar = 5 μm).

(B) Concentration of poly(GP) in cultured cortical neurons derived from individual C9BAC or Ntg littermate embryos measured by immunoassay (mean ± SEM, Ntg n = 2, C9BAC n = 6, unpaired t test).

(C) No significant differences were detected in the response of cultured cortical neurons derived from individual C9BAC and Ntg embryos to the autophagy inhibitors chloroquine or 3-methyladenine (two independent experiments, individual embryos cultured; C9BAC n = 6, Ntg n = 5, percent relative to Ntg, mean ± SEM, two-way ANOVA, Bonferroni's multiple comparison, *$p < 0.05$).

(D) ddPCR analysis of all transcripts of *C9ORF72* (Vall) relative to HPRT in two independent experiments (Exp. 1. individual embryos n = 4, mean ± SEM, one-way ANOVA, Bonferroni's multiple comparison test, *$p < 0.05$, ***$p < 0.001$; Exp. 2. mixed embryo culture, n = 3, one-way ANOVA, Bonferroni's multiple comparison test, ***$p < 0.001$).

(E) Levels of the mature microRNA product (normalized to snoRNA135) of rAAV-GFP-miRC9 trended toward correlation with percent silencing of *C9ORF72* relative to rAAV-GFP from Exp. 1 (black) and Exp. 2 (blue).

(F) Levels of poly(GP) quantified by immunoassay from primary cortical neuron cultures derived from two independent experiments (Exp. 1. individual embryos n = 2, mean ± SEM, one-way ANOVA; Exp. 2. mixed embryo culture, n = 3, one-way ANOVA, Bonferroni's multiple comparison test, **$p < 0.01$).

transcripts, RNA foci and at least one of the poly(DP) RAN-translation products. Both of these readouts rely on the expression of the *C9ORF72* gene transcripts. We have therefore tested a gene therapy approach to silence expression of the *C9ORF72* transgene in our C9BAC mice. We generated recombinant adeno-associated virus (rAAV) serotype 9 expressing an artificial microRNA (miR) targeting exon three of human *C9ORF72* preceded by an eGFP reporter, under the transcriptional control of the CB-promoter and CMV-enhancer (rAAV-GFP-miRC9). For control groups, a vector expressing only the eGFP reporter was used (rAAV-GFP). We carried out two sets of experiments in DIV4 primary cortical neuron cultures (Figures 3D–3F). In the first (Exp 1), individual cultures were generated from separate C9BAC hemizygous embryos from the same litter of C9BAC mice; in the second (Exp 2), all transgenic embryos from a C9BAC litter were pooled to generate a mixed population of cortical neurons from multiple transgenic embryos. In both experiments, at DIV10 transgene transcripts and poly(GP) were reduced by expression of the GFP control vector alone, in conjunction with some cell death; to account for this non-specific silencing, all silencing outcomes are normalized to this GFP control. In all experiments, we consistently observed further depletion of *C9ORF72* products in groups expressing the microRNA. Relative to the rAAV-GFP group, *C9ORF72* mRNA transcript (Figure 3D) expression in individual embryo cultures (Exp 1) was decreased by 35% by rAAV-GFP-miRC9 (n = 4, one-way ANOVA, Bonferroni's multiple comparison, $p < 0.05$) and 24% in the pooled embryo cultures in Exp 2 (not statistically significant; n = 3, one-way ANOVA, Bonferroni's multiple comparison). We detected mature miRNA only in the rAAV-GFP-miRC9-treated cultures and found that the percent silencing was proportional to levels of the expressed miRNA (Figure 3E).

In two cultures derived from individual embryos (Exp 1), rAAV-GFP-miRC9 reduced levels of poly(GP) by ~60% (Figure 3F). In mixed cultures (Exp 2), poly(GP) was reduced by 73% relative to GFP. Though not significant by one-way ANOVA (n = 3, Bonferroni multiple comparison test), we note that in Exp 2 statistical testing of the rAAV-GFP versus rAAV-GFP-miRC9 (independent of the untreated group) detected a significant decrease in poly(GP) levels (unpaired t test, p = 0.0008).

DISCUSSION

We report here a novel line of transgenic mice that harbor a portion of the human *C9ORF72* gene with an expanded GGGGCC repeat motif. Though the mice do not develop an overt motor phenotype, they recapitulate distinctive histopathological features seen in c9ALS/FTD patients, including both sense and antisense intranuclear RNA foci and the presence of RAN translated DPR proteins. These data indicate that the 300–500 GGGGCC repeat motifs are sufficient for the generation and deposition of abnormal tracts of RNA and DPR proteins but not to induce neurodegeneration. Why this is the case remains unclear. Possibly the pathology, seen quite clearly at the molecular level, is not sufficient to compromise motor neuron viability within the lifespan of the mice. Alternatively, some other aspect of the model may be required to induce motor pathology. For example, if the pathology in humans entails sequestration of critical RNA binding proteins by intranuclear RNA aggregates, it is possible that these proteins are more abundant in the mouse and thus less prone to be titrated to insufficiency in the RNA foci. Alternatively, it is possible that the DPR proteins are better tolerated in some manner in the mouse. Of note, in this same issue of *Neuron*, O'Rourke et al. report that an independently generated BAC transgenic mouse carrying the full human *C9ORF72* gene with the disease-associated expansion also expresses histopathological features of *C9ORF72* without behavioral abnormalities and neurodegeneration (O'Rourke et al., 2015).

Two aspects of the histological findings in these mice are intriguing. First, there were distinctly more cells containing sense foci than antisense RNA foci. This is broadly analogous to data from human cortex (Mizielinska et al., 2013). It is also conceivable that the relative paucity of antisense RNA foci reflects the structure of the human BAC in our mice, which contains the full 5′ expanse of the *C9ORF72* locus but only extends through exons 1–6 and thus might lack 3′ regulatory regions necessary for generating antisense foci. Also of interest in the C9BAC mice were age-dependent changes in the abundance of RNA foci and the levels of soluble RAN translated poly(GP) proteins. Our data indicate that the numbers of intranuclear foci composed of *C9ORF72* RNA sense transcripts declined between 10 and 24 months, possibly reflecting an age-dependent increase in clearance of these foci, reduced expression of the offending transcripts with age, or loss of foci-containing cells.

There were also age-related shifts in the properties of poly(GP) DPR proteins. In 4-month-old C9BAC mice, SDS-soluble poly(GP) species were present at a concentration comparable to levels detected in frontal cortex of some c9ALS patients. Soluble poly(GP) levels in 24-month-old C9BAC mice were lower, a change that coincided with an increased presence of poly(GP)-positive inclusions, suggesting conversion of soluble poly(GP) into insoluble, aggregating species.

Finally, we note that although the C9BAC mouse does not develop a discernible abnormal behavioral phenotype, the histopathological and transcript variant expression profile matches well with that of c9ALS/FTD patients. In successful experiments in vivo and in vitro (Donnelly et al., 2013; Lagier-Tourenne et al., 2013; Sareen et al., 2013), the *C9ORF72* expression has been reduced following treatment with antisense oligonucleotides (ASOs). In the present study, we have conducted a proof-of-principle experiment to test whether an artificial microRNA (miR) targeting exon 3 of *C9ORF72* delivered by recombinant adeno-associated virus (rAAV) might offer an alternative therapeutic strategy. With this intervention, primary cortical neuron cultures from the C9BAC transgenic mice demonstrated a consistent trend toward reduced expression of *C9ORF72* transcripts and decreased production of the poly(GP) DPR. These studies suggest that this strategy (AAV-mediated delivery of an artificial miR) merits further investigation and that these C9BAC mice will be useful for assessing therapies that silence transcription or RAN translation across the expanded GGGGCC repeats or otherwise inhibit the formation of RNA foci and DPR proteins. Combined with accurate analytical techniques to quantify levels of aberrant RNA transcripts, RNA foci, and DPR proteins, the C9BAC mouse will be of considerable use for investigating the pathophysiology of *C9ORF72*-mediated neurodegeneration and much needed therapeutic approaches.

EXPERIMENTAL PROCEDURES

Generation of *C9ORF72* Transgenic Mice

A BAC library was generated from a familial FTD/ALS patient from a *C9ORF72*-linked ALS/FTD pedigree. Transgenic animals (C9BAC) were produced using a BAC carrying a 153.2 kb genomic DNA fragment including 140.5 kb upstream of *C9ORF72*, exons 1 to exon 6 of the *C9ORF72* gene, including part of the 3′ UTR of the short isoform V1 and ~500 GGGGCC motifs between exons 1 and 2. The University of Massachusetts Medical School Institutional Animal Care and Use Committee approved all experiments involving animals.

Electrophysiological Recordings

MUNE electrophysiological recordings were as described (Xia et al., 2010). Further details and description of whole-cell cortical neuron recordings are described in the Supplemental Experimental Procedures.

Droplet Digital PCR

Frozen tissue samples were homogenized in a gentleMACS Dissociator (Miltenyi Biotec) before total RNA extraction with Trizol (Life Technologies). Reverse transcription to cDNA was performed using random hexamers and MultiScribe reverse transcriptase (High capacity RNA-to-cDNA Kit, Life Technologies). Droplet Digital PCR (ddPCR) was performed using ddPCR Supermix for Probes the QX100 Droplet Digital PCR system (Bio-Rad).

Poly(GP) Immunoassay and Immunostaining

Immunostaining and immunoassay for poly(GP) dipeptides was performed as published (Ash et al., 2013). (Details are in the Supplemental Experimental Procedures.)

Human Tissues

Frozen frontal cortex tissues analyzed for for poly(GP) via ELISA assay were obtained from the Brain Bank for Neurodegenerative Disorders at Mayo Clinic

in Jacksonville, Florida, which operates under protocols approved by the Mayo Clinic Institutional Review Board, in accordance with Health Insurance Portability and Accountability Act guidelines. Frozen frontal cortex tissues for ddPCR were obtained from the UCLA Human Brain and Spinal Fluid Resource center and University of Massachusetts and were collected under protocols approved by the UMMS Institutional Review Board.

RNA Fluorescence In Situ Hybridization

Frozen sections were hybridized overnight at 55°C with DNA probes against *C9ORF72* sense (GGCCCC) and antisense (GGGGCC) transcripts, with a Cy3 5′ end tag, followed by incubation with primary antibodies, followed by Alexa Fluor 488-conjugated secondary antibodies as required.

RNA-Seq

RNA sequencing (RNA-seq) was performed on frontal cortex tissue of 6-month-old C9BAC mice and their Ntg littermates (see Supplemental Experimental Procedures). RNA-seq data are deposited in the NCBI GEO repository (GEO: GSE74973).

MicroRNA Design and Cloning

A 22-nucleotide artificial miRNA (targeting sequence 5′-AATGCAGAGAGTGGTGCTATA-3′) in exon 3 of the *C9ORF72* gene was designed and cloned into the miR-155 backbone. This artificial miR was cloned into the 3′ UTR of a GFP encoding AAV proviral plasmid under the control of the chicken beta actin (CB) promoter with a CMV enhancer. The plasmid was used to package pseudotyped rAAV9 vectors. Plasmids and vectors can be requested for academic use at http://www.umassmed.edu/muellerlab.

ACCESSION NUMBER

The accession number for the RNA-seq data reported in this paper is GEO: GSE74973.

SUPPLEMENTAL INFORMATION

Supplemental Information includes Supplemental Experimental Procedures, three figures, and one table and can be found with this article online at http://dx.doi.org/10.1016/j.neuron.2015.11.018.

AUTHOR CONTRIBUTIONS

Conceptualization: R.H.B., O.M.P., C.M., G.T.C., H.T., H.R.H. Methodology: R.H.B., O.M.P., S.P.B., G.T.C., C.M., C.J., P.d.J., L.P., T.F.G., H.T., P.C.S. Investigation: O.M.P., G.T.C., H.T., J.E.M., S.P.B., J.K., Z.K., J.M., A.W., L.P., T.F.G., L.D., Y.-J.Z., J.S., N.W., Z.L., H.S. Resources: K.B.B., D.D. Writing – Original Draft: R.H.B., O.M.P. Writing – Review & Editing: G.T.C, C.M., H.T., T.F.G., H.R.H., F.-B.G. Supervision: R.H.B., O.M.P., C.M., P.C.S., T.F.G. Funding Acquisition: R.H.B., C.M., L.P., H.R.H.

ACKNOWLEDGMENTS

The authors gratefully acknowledge the ALS Association, which funded the generation of these C9BAC mice as well as the ALS/FTD ALS genetics consortium (Lucie Bruijn, Bob Brown, Jonathan Haines, Chris Shaw, Teepu Siddique, and Peggy Vance), which provided the *C9ORF72* BAC used in this study. We are grateful to Pin-Tsun Lee for assistance with behavioral testing; the UMass Medical School Electron Microscopy Core Facility, and Kevin Kenna, Elisa Donnard, and the UMASS bioinformatics core for helpful discussions; and Zuoshang Xu and Chunxing Yang for generously supplying antibodies to TDP-43 protein. R.H.B. and C.M. are consultants for Voyager, which did not fund or otherwise participate in this study. They are inventors on a patent filed for the use of rAAV mediated silencing of *C9ORF72*. L.P. and T.G. have licensed for distribution an antibody to the poly(GP) dipeptide. This work was supported by the National Institutes of Health/National Institute of Neurological Disorders and Stroke R01NS088689 (R.H.B., L.P., C.M., O.M.P.), R21NS089979 (T.F.G.), R01 NS057553 (F.-B.G.), R21NS084528 (L.P.), R01NS063964 (L.P.); R01NS077402 (L.P.); P01NS084974 (L.P.), R01FD004127 (R.H.B.), R01NS079836 (R.H.B.), R01NS065847 (R.H.B.), R01NS073873 (R.H.B.), National Institute of Environmental Health Services R01ES20395 (L.P.), Department of Defense ALSRP AL130125 (L.P.), Mayo Clinic Foundation (L.P.), Mayo Clinic Center for Individualized Medicine (L.P.), ALS Association (R.B., L.P., T.F.G.), Robert Packard Center for ALS Research at Johns Hopkins (L.P., F.-B.G.), Target ALS (L.P., J.K., S.P.B.), ALS Therapy Alliance (F.-B.G., R.H.B.), Grant OD018259 (C.M.), the Angel Fund (R.H.B.), Project ALS (R.H.B.), and the Max Rosenfeld Fund (R.H.B., O.M.P.). H.T. is a Milton Safenowitz Postdoctoral Fellow funded by the ALS Association. O.M.P. is supported by the Michael J. Fox Foundation. J.K. is supported by a National Research Foundation of Korea Fellowship (NRF-2011-357-E00005). S.P.B. is supported by a Klingenstein-Simons Fellowship in the Neurosciences. P.C.S. is supported through the auspices of H.R.H., an Investigator at the Howard Hughes Medical Institute.

Received: February 26, 2015
Revised: October 14, 2015
Accepted: November 13, 2015
Published: December 2, 2015

REFERENCES

Alfieri, J.A., Pino, N.S., and Igaz, L.M. (2014). Reversible behavioral phenotypes in a conditional mouse model of TDP-43 proteinopathies. J. Neurosci. *34*, 15244–15259.

Almeida, S., Gascon, E., Tran, H., Chou, H.J., Gendron, T.F., Degroot, S., Tapper, A.R., Sellier, C., Charlet-Berguerand, N., Karydas, A., et al. (2013). Modeling key pathological features of frontotemporal dementia with C9ORF72 repeat expansion in iPSC-derived human neurons. Acta Neuropathol. *126*, 385–399.

Ash, P.E., Bieniek, K.F., Gendron, T.F., Caulfield, T., Lin, W.L., Dejesus-Hernandez, M., van Blitterswijk, M.M., Jansen-West, K., Paul, J.W., 3rd, Rademakers, R., et al. (2013). Unconventional translation of C9ORF72 GGGGCC expansion generates insoluble polypeptides specific to c9FTD/ALS. Neuron *77*, 639–646.

Belzil, V.V., Bauer, P.O., Prudencio, M., Gendron, T.F., Stetler, C.T., Yan, I.K., Pregent, L., Daughrity, L., Baker, M.C., Rademakers, R., et al. (2013). Reduced C9orf72 gene expression in c9FTD/ALS is caused by histone trimethylation, an epigenetic event detectable in blood. Acta Neuropathol. *126*, 895–905.

Chew, J., Gendron, T.F., Prudencio, M., Sasaguri, H., Zhang, Y.J., Castanedes-Casey, M., Lee, C.W., Jansen-West, K., Kurti, A., Murray, M.E., et al. (2015). Neurodegeneration. C9ORF72 repeat expansions in mice cause TDP-43 pathology, neuronal loss, and behavioral deficits. Science *348*, 1151–1154.

Ciura, S., Lattante, S., Le Ber, I., Latouche, M., Tostivint, H., Brice, A., and Kabashi, E. (2013). Loss of function of C9orf72 causes motor deficits in a zebrafish model of amyotrophic lateral sclerosis. Ann. Neurol. *74*, 180–187.

Cooper-Knock, J., Walsh, M.J., Higginbottom, A., Robin Highley, J., Dickman, M.J., Edbauer, D., Ince, P.G., Wharton, S.B., Wilson, S.A., Kirby, J., et al. (2014). Sequestration of multiple RNA recognition motif-containing proteins by C9orf72 repeat expansions. Brain *137*, 2040–2051.

DeJesus-Hernandez, M., Mackenzie, I.R., Boeve, B.F., Boxer, A.L., Baker, M., Rutherford, N.J., Nicholson, A.M., Finch, N.A., Flynn, H., Adamson, J., et al. (2011). Expanded GGGGCC hexanucleotide repeat in noncoding region of C9ORF72 causes chromosome 9p-linked FTD and ALS. Neuron *72*, 245–256.

Donnelly, C.J., Zhang, P.W., Pham, J.T., Haeusler, A.R., Mistry, N.A., Vidensky, S., Daley, E.L., Poth, E.M., Hoover, B., Fines, D.M., et al. (2013). RNA toxicity from the ALS/FTD C9ORF72 expansion is mitigated by antisense intervention. Neuron *80*, 415–428.

Farg, M.A., Sundaramoorthy, V., Sultana, J.M., Yang, S., Atkinson, R.A., Levina, V., Halloran, M.A., Gleeson, P.A., Blair, I.P., Soo, K.Y., et al. (2014). C9ORF72, implicated in amytrophic lateral sclerosis and frontotemporal dementia, regulates endosomal trafficking. Hum. Mol. Genet. *23*, 3579–3595.

Gascon, E., Lynch, K., Ruan, H., Almeida, S., Verheyden, J.M., Seeley, W.W., Dickson, D.W., Petrucelli, L., Sun, D., Jiao, J., et al. (2014). Alterations in microRNA-124 and AMPA receptors contribute to social behavioral deficits in frontotemporal dementia. Nat. Med. *20*, 1444–1451.

Geevasinga, N., Menon, P., Nicholson, G.A., Ng, K., Howells, J., Kril, J.J., Yiannikas, C., Kiernan, M.C., and Vucic, S. (2015). Cortical function in asymptomatic carriers and patients with C9orf72 amyotrophic lateral sclerosis. JAMA Neurol. *72*, 1268–1274.

Gijselinck, I., Van Langenhove, T., van der Zee, J., Sleegers, K., Philtjens, S., Kleinberger, G., Janssens, J., Bettens, K., Van Cauwenberghe, C., Pereson, S., et al. (2012). A C9orf72 promoter repeat expansion in a Flanders-Belgian cohort with disorders of the frontotemporal lobar degeneration-amyotrophic lateral sclerosis spectrum: a gene identification study. Lancet Neurol. *11*, 54–65.

Janssens, J., and Van Broeckhoven, C. (2013). Pathological mechanisms underlying TDP-43 driven neurodegeneration in FTLD-ALS spectrum disorders. Hum. Mol. Genet. *22* (R1), R77–R87.

Lagier-Tourenne, C., Baughn, M., Rigo, F., Sun, S., Liu, P., Li, H.R., Jiang, J., Watt, A.T., Chun, S., Katz, M., et al. (2013). Targeted degradation of sense and antisense C9orf72 RNA foci as therapy for ALS and frontotemporal degeneration. Proc. Natl. Acad. Sci. USA *110*, E4530–E4539.

Majounie, E., Renton, A.E., Mok, K., Dopper, E.G., Waite, A., Rollinson, S., Chiò, A., Restagno, G., Nicolaou, N., Simon-Sanchez, J., et al.; Chromosome 9-ALS/FTD Consortium; French research network on FTLD/FTLD/ALS; ITALSGEN Consortium (2012). Frequency of the C9orf72 hexanucleotide repeat expansion in patients with amyotrophic lateral sclerosis and frontotemporal dementia: a cross-sectional study. Lancet Neurol. *11*, 323–330.

Mizielinska, S., and Isaacs, A.M. (2014). C9orf72 amyotrophic lateral sclerosis and frontotemporal dementia: gain or loss of function? Curr. Opin. Neurol. *27*, 515–523.

Mizielinska, S., Lashley, T., Norona, F.E., Clayton, E.L., Ridler, C.E., Fratta, P., and Isaacs, A.M. (2013). C9orf72 frontotemporal lobar degeneration is characterised by frequent neuronal sense and antisense RNA foci. Acta Neuropathol. *126*, 845–857.

Mori, K., Weng, S.M., Arzberger, T., May, S., Rentzsch, K., Kremmer, E., Schmid, B., Kretzschmar, H.A., Cruts, M., Van Broeckhoven, C., et al. (2013). The C9orf72 GGGGCC repeat is translated into aggregating dipeptide-repeat proteins in FTLD/ALS. Science *339*, 1335–1338.

O'Rourke, J.G., Bogdanik, L., Muhammad, A.K.M.G., Gendron, T.F., Kim, K.J., Austin, A., Cady, J., Liu, E.Y., Zarrow, J., Grant, S., et al. (2015). *C9orf72* BAC transgenic mice display typical pathologic features of ALS/FTD. Neuron *88*, this issue, 892–901.

Prudencio, M., Belzil, V.V., Batra, R., Ross, C.A., Gendron, T.F., Pregent, L.J., Murray, M.E., Overstreet, K.K., Piazza-Johnston, A.E., Desaro, P., et al. (2015). Distinct brain transcriptome profiles in C9orf72-associated and sporadic ALS. Nat. Neurosci. *18*, 1175–1182.

Renton, A.E., Majounie, E., Waite, A., Simón-Sánchez, J., Rollinson, S., Gibbs, J.R., Schymick, J.C., Laaksovirta, H., van Swieten, J.C., Myllykangas, L., et al.; ITALSGEN Consortium (2011). A hexanucleotide repeat expansion in C9ORF72 is the cause of chromosome 9p21-linked ALS-FTD. Neuron *72*, 257–268.

Rohrer, J.D., Isaacs, A.M., Mizielinska, S., Mead, S., Lashley, T., Wray, S., Sidle, K., Fratta, P., Orrell, R.W., Hardy, J., et al. (2015). C9orf72 expansions in frontotemporal dementia and amyotrophic lateral sclerosis. Lancet Neurol. *14*, 291–301.

Sareen, D., O'Rourke, J.G., Meera, P., Muhammad, A.K., Grant, S., Simpkinson, M., Bell, S., Carmona, S., Ornelas, L., Sahabian, A., et al. (2013). Targeting RNA foci in iPSC-derived motor neurons from ALS patients with a C9ORF72 repeat expansion. Sci. Transl. Med. *5*, 208ra149.

Therrien, M., Rouleau, G.A., Dion, P.A., and Parker, J.A. (2013). Deletion of C9ORF72 results in motor neuron degeneration and stress sensitivity in C. elegans. PLoS ONE *8*, e83450.

Tran, H., Almeida, S., Moore, J., Gendron, T.F., Chalasani, U., Lu, Y., Du, X., Nickerson, J.A., Petrucelli, L., Weng, Z., et al. (2015). Differential Toxicity of Nuclear RNA Foci versus Dipeptide Repeat Proteins in a Drosophila Model of C9ORF72 FTD/ALS. Neuron *87*, 1207–1214.

Xia, R.H., Yosef, N., and Ubogu, E.E. (2010). Dorsal caudal tail and sciatic motor nerve conduction studies in adult mice: technical aspects and normative data. Muscle Nerve *41*, 850–856.

Zu, T., Gibbens, B., Doty, N.S., Gomes-Pereira, M., Huguet, A., Stone, M.D., Margolis, J., Peterson, M., Markowski, T.W., Ingram, M.A., et al. (2011). Non-ATG-initiated translation directed by microsatellite expansions. Proc. Natl. Acad. Sci. USA *108*, 260–265.